Calcium Flickers Steer Cell Migration

Chaoliang Wei[1], **Xianhua Wang**[1], **Min Chen**[1], **Kunfu Ouyang**[1], **Long-Sheng Song**[2], and **Heping Cheng**[1]

[1]Institute of Molecular Medicine, National Laboratory of Biomembrane and Membrane Biotechnology, Peking University, Beijing 100871, China

[2]Department of Internal Medicine, Division of Cardiovascular Medicine, University of Iowa Carver College of Medicine, Iowa City 52242, Iowa, USA

Abstract

Directional movement is a property common to all cell types during development and is critical to tissue remodelling and regeneration after damage[1–3]. In migrating cells, calcium plays a multifunctional role in directional sensing, cytoskeleton redistribution, traction force generation, and relocation of focal adhesions[1, 4–7]. Here we visualise, for the first time, high-calcium microdomains ("calcium flickers"), and their patterned activation in migrating fibroblasts. Calcium flicker activity is dually coupled to membrane tension (*via* TRPM7, a stretch-activated Ca^{2+}-permeant channel of the transient receptor potential superfamily[8]) and chemoattractant signal transduction (*via* type 2 inositol 1,4,5-trisphosphate receptors). Interestingly, calcium flickers are most active at the leading lamella of migrating cells, displaying a 4:1 front-to-rear polarisation opposite to the global calcium gradient[6]. When exposed to a PDGF gradient perpendicular to cell movement, asymmetric calcium flicker activity develops across the lamella and promotes the turning of migrating fibroblasts. These findings illustrate how the exquisite spatiotemporal organisation of calcium microdomains can orchestrate complex cellular processes such as cell migration.

In addition to extracellular chemoattractant stimuli, directional cell movement depends on an intracellular calcium signal that is well-organised in space, time and concentration[6, 7, 9]. Over a decade ago, Fay and colleagues made the groundbreaking finding that intracellular calcium displays a rear-to-front gradient, with the lowest concentration at the front of a migrating cell[6]. However, this observation appears to be paradoxical, because the leading lamella, the signalling and motility centre of a migrating cell, contains numerous effector proteins that require high levels of calcium for activation[10–13]. Although transient increases of calcium concentration have recently been observed in migrating cells, they are infrequent and mainly localised to the tail of the cell, and are thought to facilitate intermittent rear retraction[7]. Biochemical studies suggest that calcium entry is required to maintain ruffling structure, actin polymerisation, and the phosphatidylinositol-3,4,5-trisphosphate (PIP_3) signalling at the leading edge of macrophages[14]. To date, it remains perplexing how calcium regulates lamella dynamics during cell migration.

Using human embryonic lung fibroblasts (WI-38) as a model, we characterised the spatiotemporal organisation of intracellular calcium signals with the aid of real-time confocal microscopy. In migrating WI-38 fibroblasts that overtly displayed leading and trailing edges, we detected a shallow decreasing gradient of global calcium concentration (indexed by the fluo-4 to fura-red fluorescence ratio) that ran from the rear to the front (Fig.

Address Editorial Correspondence to Heping Cheng, Ph.D., Institute of Molecular Medicine, Peking University, Beijing 100871, China, +86-10-6276-5957 (phone/fax), chengp@pku.edu.cn and C.W. (chaoliang.wei@gmail.com).

1c, d), in agreement with previous findings[6, 9]. Surprisingly, we found that discrete, local and short-lived high-calcium microdomains or "calcium flickers", analogous to calcium sparks and puffs[15], occurred against a quiescent background (supplementary video). High resolution linescan imaging revealed that the flickers occurred at a nearly constant rate of 1.92 ± 0.21 Hz/100 μm linescan (n = 18) (Fig. 1c). Individual events rapidly rose to about double the fluo-4 fluorescence ($\Delta F/F_o = 1.16 \pm 0.02$, n = 1,071), lasting variably from 10 ms to 4 s, and were confined to an area 5.27 ± 0.05 μm in diameter (Fig. 1c). Importantly, calcium flickers were abundant at the leading lamella (Fig. 1a), including in motile lamellipodia (Fig. 1b), but were sharply reduced elsewhere, resulting in an approximately 4:1 front-to-rear polarisation (Fig. 1d) that was opposite to the aforementioned global calcium gradient. Polarisation of flicker activity was common to fibroblasts undergoing migration, but it was not seen in stationary fibroblasts lacking morphological polarity and displaying a lower flicker incidence (0.57 ± 0.10 Hz/100 μm linescan, n = 12, p < 0.05 *vs.* migrating cells) (supplementary Fig. 1). Thus, flickers represent a distinctive, heretofore unappreciated modality of calcium signalling in migrating fibroblasts. Similar flickers were also evident in rat neonatal cardiac fibroblasts and 3T3-Swiss albino mouse embryonic fibroblasts (supplementary Fig. 2).

In search of the molecular basis of calcium flickers, we showed that calcium influx through the stretch-activated cation channel (SACC) was obligatory. Application of Ca^{2+}-free medium containing 5 mM EGTA or streptomycin (200 μM), a SACC blocker[16], immediately abolished flicker activity in WI-38 fibroblasts (Fig. 2a). On average, the signal mass of calcium flickers (space-time integral of the flicker signal) decreased by $98.3 \pm 0.8\%$ (EGTA; n = 9, p < 0.01 *vs.* control) or $93.1 \pm 1.3\%$ (streptomycin; n = 6, p < 0.01 *vs.* control). Likewise, Gd^{3+} (200 μM), a non-specific SACC blocker[16], diminished the signal mass by $91.9 \pm 1.2\%$ (n = 6, p < 0.01 *vs.* control). To determine whether mechanical forces can directly trigger flickers, we showed that shear stress applied to the front of migrating fibroblasts immediately evoked a flurry of flicker activity (Fig. 2e). In a different approach, relaxing or stretching the cell by pushing or pulling the flexible substrate (with a needle tip) suppressed or enhanced the flicker activity, respectively (supplementary Fig. 3). Under cell-attached patch clamp conditions[17], sudden application of negative pressure (~40 mm Hg) elicited bursting single-channel activity, while simultaneous confocal imaging visualised corresponding flicker-like events beneath the patch membrane (Fig. 2b). These results indicate that calcium flickers are triggered by calcium influx through SACCs.

SACCs belong to the transient receptor potential (TRP) ion channel superfamily. In mammals, about eight TRP channels in four subfamilies are thought to be sensitive to mechanical forces while being calcium-permeable[8]. Of these, TRPM7, TRPC6, TRPV2 and TRPP2 were expressed at relatively high mRNA levels in WI-38 fibroblasts (supplementary Fig. 4). Using RNA interference, we found that calcium flickers were virtually abolished by ~75% knockdown of TRPM7, but not that of the other three TRP channels (Fig. 2c, d, supplementary Fig. 5). More importantly, similar shear stress was unable to evoke flickers in TRPM7 knockdown cells, which displayed rare basal flicker activity (Fig. 2e). These data pinpointed TRPM7 as the specific SACC responsible for transducing mechanical signals into calcium flickers. A hallmark of TRPM7 is its sensitivity to inhibition by Mg^{2+} in addition to Gd^{3+} [18]. Raising extracellular Mg^{2+} from 1.0 to 10 mM largely abolished calcium flickers, while removing it enhanced flicker production (supplementary Fig. 6). Thus, TRPM7 acts as the mechanical sensor, the calcium flicker igniter, and the mechanochemical transducer in fibroblasts, revealing a novel role of this SACC in the regulation of cell migration (see below).

Since calcium release from the endoplasmic reticulum (ER) amplifies calcium influxes *via* the calcium-induced calcium release mechanism[15], we next investigated whether ER

calcium release participates in calcium flicker production. Inhibition of ER calcium recycling with the Ca^{2+} ATPase inhibitor thapsigargin (5 μM, 20 min incubation, after recession of the initial calcium transient) halved flicker amplitude without affecting flicker probability (Fig. 3a, c). Similar results were obtained by inhibiting the IP_3 receptor (IP_3R) with xestospongin C (5 μM), whereas IP_3-BM (2 μM), a membrane-permeable ester precursor of IP_3[19], enhanced the flicker amplitude and ryanodine receptor inhibition (ryanodine, 25 μM) had no significant effect (Fig. 3a, c). Quantitative real-time PCR results showed that type 2 IP_3R (IP_3R2) and type 3 IP_3R (IP_3R3) are the primary IP_3R isoforms expressed in WI-38 fibroblasts (supplementary Fig. 7). In contrast to TRPM7, RNA interference knockdown of IP_3R2 (~80%), but not IP_3R3 (~60%), significantly decreased flicker amplitude but failed to alter flicker probability (Fig. 3b, c). This IP_3R isoform specificity is consistent with the fact that IP_3R2 is more sensitive to IP_3 and displays little calcium-dependent inactivation[20]. Taking together, we concluded that calcium entry *via* TRPM7 is locally amplified by calcium release through IP_3R2 in the event of a calcium flicker. Coupling IP_3R2 to TRPM7 would enable flicker activity to decode IP_3-linked chemoattractant signal transduction.

Given the role of TRPM7 as a mechanical sensor and a calcium flicker igniter, we anticipated that flicker activity would be coupled to the migration-associated traction force. Indeed, the map of flicker ignition sites at the front of a cell largely overlapped, though with subtle differences, the matrix of focal adhesions (FAs) (Fig. 4a, supplementary Fig. 8), where traction force is created and transmitted[21]. Rapid local application of RGDS (2 mM, 1 min), which contains the RGD sequence that is recognized by integrins[22], enhanced the flicker activity, while the control peptide RGES was ineffective (Fig. 4b, c), consistent with the finding that RGDS stimulates calcium transients in neuronal filopodia and growth cones[23]. Disruption of protrusion by transient frontal application of cytochalasin D, inhibition of myosin ATPase by 2,3-butanedione monoxime or (−)blebbistatin[24] all inhibited lamella flicker production (Fig. 4b, c). These lines of evidence support the idea that decoding local membrane tension by flicker activity depends on cytoskeletal and morphological integrity.

Despite the low global calcium concentration, high-calcium microdomains created by mechanical stress in the leading lamella may activate a multitude of local calcium-dependent events critical to cell polarization and movement, including the PIP_3 signalling cascade[25, 26], a parallel phospholipase A2-mediated signalling mechanism[27], cytoskeleton dynamic such as actin remodelling[10], FA detachment and relocation, and actin-myosin contraction. Next, we sought to determine the physiological role of calcium flickers in regulating cell migration, particularly turning behaviour that is almost entirely carried out within the leading lamella.

Platelet derived growth factor (PDGF) is a well-known chemoattractant that stimulates fibroblast migration during wound healing[3]. Its intracellular signalling pathways include generating traction force by Rac-dependent protrusion[28] and activation of the phospholipase C-PIP_2-IP_3 signaling cascade[29], both convergent on flicker production. When migrating fibroblasts were exposed to uniform PDGF (0.8 nM), increases in both flicker amplitude and probability were accompanied by a decrease in directional persistence (supplementary Fig. 9), the latter suggesting an enhanced propensity for turning of the cell[30]. When a PDGF gradient was applied in the direction perpendicular to cell movement, migrating fibroblasts no longer moved persistently along the original path; rather, they turned towards the higher PDGF concentration (Fig. 5a). Time-lapse imaging revealed a rapid increase in lamella flicker activity and an accentuated front-to-rear polarisation (Fig. 5a). More importantly, a greater flicker signal mass was found in the portion facing the PDGF source (SM_α) than in the portion farther away from the source (SM_β), indicating the development of an

asymmetry of flicker activity within the lamella (Fig. 5a). To demonstrate a linkage between lamella flicker asymmetry and turning behaviour, we examined the cumulative difference between SM_α and SM_β ($\Sigma SM_{\alpha\text{-}\beta}$) and found that the time course of $\Sigma SM_{\alpha\text{-}\beta}$ nearly overlapped with that for the distance travelled in the direction of the PDGF gradient (y-distance) (Fig. 5b). On average, the correlation coefficient between $\Sigma SM_{\alpha\text{-}\beta}$ and y-distance was 0.72 in 25 migrating fibroblasts. Hence, patterned flicker activation in the leading lamella may translate directional sense and steer the cell to turn in response to PDGF gradients.

To further test the above hypothesis, we showed that impaired PDGF-induced lamella flicker asymmetry or diminishment of $\Sigma SM_{\alpha\text{-}\beta}$ by streptomycin and TRPM7 or IP$_3$R2 knockdown was accompanied by dwindling of the turning angle in a roughly proportional manner (Fig. 5c). Likewise, a robust match between the flicker activity and population chemotaxis was revealed by various pharmacological and molecular interventions including TRPM7 and IP$_3$R2 knockdown, and SACC blockade (Fig. 5d, supplementary Fig. 10). Furthermore, loading EGTA ester to disturb the flicker signal (supplementary Fig. 11) compromised the turning and chemotaxis abilities (Fig. 5c, d), while flicker activation by IP$_3$-BM enhanced both of them (Fig. 5c, d), suggesting a causal link between calcium flicker activity and fibroblast turning and chemotaxis.

In summary, we have demonstrated that calcium flickers arising from TRPM7 and IP$_3$R2 play an essential role in steering migrating fibroblasts. Despite that the global calcium gradient is opposite to the direction of cell migration, high calcium flicker activity would enable activation of calcium signalling cascades amidst a low calcium background at the leading edge, such that spatiotemporally patterned calcium flicker activity can orchestrate the complex turning behaviour of migrating cells (Fig. 5e). The coupling of TRPM7-mediated force-transducing calcium influx and local IP$_3$-induced calcium release would make this an ideal system for locomotion in response to chemoattractants (Fig. 5e). The present finding may have general ramifications because growth cones of neurons turn away from the side which filopodia displays higher local calcium signals[23] and calcium influx is essential to maintaining the leading-edge structure and activity in macrophages[14]. As such, unveiling calcium flickers in migrating cells opens a new avenue to investigate how local calcium signals orchestrate diverse biochemical pathways in the guidance of directional movement.

Methods

Cell Culture

Human lung embryonic WI-38 fibroblasts (21 population doublings, PDs) obtained from the American Type Culture Collection were maintained and subcultured to 28 PDs in MEM (Gibco) supplemented with 10% FBS (Hyclone), 2 mM glutamine and 200 units/ml penicillin in a 37°C, 5% CO$_2$ incubator. For functional experiments, cells were plated at a density of 1×10^4/cm^2 and cultured for 10 h on coverslips coated with 5 μg/ml fibronectin (Sigma).

Calcium Imaging

WI-38 cells were loaded with fluo-4 AM (5 μM) alone or in combination with fura-red AM (5 μM) for 6 min at 37°C, rinsed twice, and then bathed in Hepes-buffered saline solution containing (in mM): 134 NaCl, 5.4 KCl, 1.0 MgSO$_4$, 1.0 NaH$_2$PO$_4$, 1.8 CaCl$_2$, 20 Hepes, and 5 D-glucose (pH 7.4) with 1% FBS, unless otherwise specified. Cells were placed in a 37°C heated chamber (Zeiss S-Type incubator) and imaged on a Zeiss LSM 510 confocal microscope with a 40× oil objective (NA 1.3) at radial and axial resolutions of 0.4 and 1.0

µm, respectively. For ratiometric imaging, cells were excited at 488 nm, emission was detected at 505–550 nm (fluo-4 signal) and >633 nm (fura-red signal), and DIC transmission image was acquired simultaneously. For migration path analysis and calcium flicker signal mass measurement, 300–600 time-lapse images were acquired at 6 s intervals. High resolution linescan imaging of calcium flickers was performed at 3 ms per linescan.

PCR

Total RNA was isolated from 28PDs WI-38 fibroblasts with TRI Reagent (Sigma) and converted to cDNA by using M-MLV reverse transcriptase (Promega). Quantitative RT-PCR reactions were carried out using these cDNAs in an iQ5 real-time PCR detection system (BioRad). Results were read out using iQ5 optical system software. All samples showing primer dimer formation or spurious, non-specific peaks, as indicated by the dissociation curve, were excluded from analysis. The primers are shown in supplementary Table 1.

RNA Interference

RNAi sequences for IP_3R isoforms and TRP channels were designed using RNAi Designer (http://www.invitrogen.com/rnai) (supplementary Table 2). Each scrambled control was designed corresponding to first duplex of siRNA. Briefly, corresponding siRNA duplexes were synthesized (GenePharma, Shanghai or Invitrogen, USA) and transfected into cells with Lipofectamine RNAiMax (Invitrogen) according to the manufacturer's recommendations. Western blotting or functional studies were carried out 72 hours after transfection.

Western Blotting

Total protein extracted from WI-38 cells with siRNA treatment was separated on 4–12% NuPAGE Novex Bis-Tris gels (Invitrogen) and transferred to PVDF membranes (Millipore). After blocking for 1 h with 5% nonfat dry milk, the PVDF membrane was probed with primary antibody (anti-IP_3R2 is the gift of Ju Chen at UCSD; anti-IP_3R3 from Santa Cruz; anti-tubulin from Sigma; anti-TRPC6 from Millipore; anti-TRPV2 from ABR; anti-TRPP2 and anti-TRPM7 from Abcam) for 2 h at room temperature, and then secondary antibody (IRDye-conjugated anti-mouse, anti-rabbit and anti-goat IgG from LI-COR) for 1 h at room temperature. Immunoblots were detected using the Odyssey imaging system.

Cell Migration Analysis

Fibroblasts with an overt leading lamella and a thin trailing edge were selected for migration analysis. The outer boundary of the cell was extracted from the respective fluorescence image for calculation of its centre of gravity. The centres of consecutive images (6 s apart) defined the trajectory of cell movement. Migration speed was calculated as the average displacement per min during 30 min. Directional persistence (D/T ratio) was calculated as the ratio between the linear displacement and the total length of the trajectory during 30 min.

To establish a PDGF-BB (PeproTech) gradient perpendicular to the long axis of a polarized migrating fibroblast, a 5 µm internal diameter, PDGF BB-containing (3 nM) micropipette was placed ~150 µm away from one side of the cell. By visualisation of sulfurhodamine fluorescence under similar conditions, we estimated an average PDGF concentration of 1 nM and an edge-to-edge difference of 0.4 nM across the leading lamella (~40 µm).

Chemotaxis Assay

24–well Transwell plates with inserts containing 8 µm pores in a polycarbonate membrane (Corning) were used for chemotaxis assays. Briefly, the outer wells contained 600 µL MEM

medium containing 1% FBS with PDGF-BB (0.8 nM) as chemoattractant. Approximately 8×10^3 overnight-starved (1% FBS) WI-38 fibroblasts in 100 µL PDGF-BB free MEM medium containing1% FBS and designated drug were added to each insert. In chemokinesis control group, PDGF-BB (0.8 nM) was also added to the insert to abolish the concentration gradient. Transwell plate was then incubated for 12 hours in a 37°C, 5% CO_2 incubator before assay.

For assay, the inserts were loaded with 5 µM calcein AM for 10 min and then fixed immediately with 3% formaldehyde for 10 min. Cells in inserts were cleared and those under the lower surface of the polycarbonate membrane were imaged and analysed.

Application of Mechanical Forces

Shear stress was locally applied by a gentle jet flow (4 cm H_2O pressure) *via* a patch pipette (10 µm internal diameter) ~80 µm away from the front of migrating fibroblasts. Note that jet flow used in local drug delivery (1 cm H_2O pressure, ~120 µm placement, pipette with 5 µm internal diameter) did not alter calcium flicker activity (n=4).

Recording SACC Currents and Imaging Local Calcium Influx

Cell-attached patch-clamp technique, using an EPC-7 amplifier (Germany), was applied to fibroblasts preloaded with the calcium indicator, fluo-4 AM. The patch pipette (2–3 MΩ) solution contained (in mM): NaCl 140, KCl 5.4, $MgCl_2$ 1.0, Hepes 20, and $CaCl_2$ 1.8 (pH 7.4, adjusted with NaOH). To activate SACCs, mechanical suction of ~40 mm Hg was applied *via* a syringe connected to the patch pipette while the patch membrane was held 80 mV more negative than the resting membrane potential to enhance Ca^{2+} entry. The single-channel currents were filtered at 3 kHz and digitised at 5 kHz with pClamp 6.0 software. Linescan images of local calcium immediately beneath the patch membrane were acquired simultaneously at 3 ms resolution.

Data Analysis

Digital image processing used IDL software (Research Systems) and custom-devised computer algorithms. Statistical data are expressed as mean ± s.e.m. Student's *t*-test and paired *t*-test were applied when appropriate. A P value less than 0.05 was considered statistically significant.

Supplementary Material

Refer to Web version on PubMed Central for supplementary material.

Acknowledgments

References

1. Ridley AJ, et al. Cell migration: integrating signals from front to back. Science. 2003; 302:1704–1709. [PubMed: 14657486]

2. Martin P, Parkhurst SM. Parallels between tissue repair and embryo morphogenesis. Development. 2004; 131:3021–3034. [PubMed: 15197160]

3. Werner S, Grose R. Regulation of wound healing by growth factors and cytokines. Physiol Rev. 2003; 83:835–870. [PubMed: 12843410]

4. Van Haastert PJ, Devreotes PN. Chemotaxis: signalling the way forward. Nat. Rev. Mol. Cell Biol. 2004; 5:626–634. [PubMed: 15366706]

5. Pettit EJ, Fay FS. Cytosolic free calcium and the cytoskeleton in the control of leukocyte chemotaxis. Physiol Rev. 1998; 78:949–967. [PubMed: 9790567]

6. Brundage RA, Fogarty KE, Tuft RA, Fay FS. Calcium gradients underlying polarization and chemotaxis of eosinophils. Science. 1991; 254:703–706. [PubMed: 1948048]

7. Lee J, Ishihara A, Oxford G, Johnson B, Jacobson K. Regulation of cell movement is mediated by stretch-activated calcium channels. Nature. 1999; 400:382–386. [PubMed: 10432119]

8. Nilius B, Owsianik G, Voets T, Peters JA. Transient receptor potential cation channels in disease. Physiol Rev. 2007; 87:165–217. [PubMed: 17237345]

9. Hahn K, DeBiasio R, Taylor DL. Patterns of elevated free calcium and calmodulin activation in living cells. Nature. 1992; 359:736–738. [PubMed: 1436037]

10. Stossel TP, Fenteany G, Hartwig JH. Cell surface actin remodeling. J. Cell Sci. 2006; 119:3261–3264. [PubMed: 16899816]

11. Robinson RC, et al. Domain movement in gelsolin: a calcium-activated switch. Science. 1999; 286:1939–1942. [PubMed: 10583954]

12. Chew TL, Wolf WA, Gallagher PJ, Matsumura F, Chisholm RL. A fluorescent resonant energy transfer-based biosensor reveals transient and regional myosin light chain kinase activation in lamella and cleavage furrows. J. Cell Biol. 2002; 156:543–553. [PubMed: 11815633]

13. Franco SJ, et al. Calpain-mediated proteolysis of talin regulates adhesion dynamics. Nat. Cell Biol. 2004; 6:977–983. [PubMed: 15448700]

14. Evans JH, Falke JJ. Ca^{2+} influx is an essential component of the positive-feedback loop that maintains leading-edge structure and activity in macrophages. Proc. Natl. Acad. Sci. U. S. A. 2007; 104:16176–16181. [PubMed: 17911247]

15. Cheng H, Lederer WJ. Calcium Sparks. Physiol Rev. 2008; 88:1491–1545. [PubMed: 18923188]

16. Hamill OP, McBride DW Jr. The pharmacology of mechanogated membrane ion channels. Pharmacol. Rev. 1996; 48:231–252. [PubMed: 8804105]

17. Zou H, Lifshitz LM, Tuft RA, Fogarty KE, Singer JJ. Visualization of Ca^{2+} entry through single stretch-activated cation channels. Proc. Natl. Acad. Sci. U. S. A. 2002; 99:6404–6409. [PubMed: 11983921]

18. Numata T, Shimizu T, Okada Y. TRPM7 is a stretch- and swelling-activated cation channel involved in volume regulation in human epithelial cells. Am. J. Physiol Cell Physiol. 2007; 292:C460–C467. [PubMed: 16943238]

19. Thomas D, et al. Microscopic properties of elementary Ca2+ release sites in non-excitable cells. Curr. Biol. 2000; 10:8–15. [PubMed: 10660296]

20. Patterson RL, Boehning D, Snyder SH. Inositol 1,4,5-trisphosphate receptors as signal integrators. Annu. Rev. Biochem. 2004; 73:437–465. [PubMed: 15189149]

21. Horwitz AR, Parsons JT. Cell migration--movin' on. Science. 1999; 286:1102–1103. [PubMed: 10610524]

22. Pierschbacher MD, Ruoslahti E. Cell attachment activity of fibronectin can be duplicated by small synthetic fragments of the molecule. Nature. 1984; 309:30–33. [PubMed: 6325925]

23. Gomez TM, Robles E, Poo M, Spitzer NC. Filopodial calcium transients promote substrate-dependent growth cone turning. Science. 2001; 291:1983–1987. [PubMed: 11239161]

24. Shu S, Liu X, Korn ED. Blebbistatin and blebbistatin-inactivated myosin II inhibit myosin II-independent processes in Dictyostelium. Proc. Natl. Acad. Sci. U. S. A. 2005; 102:1472–1477. [PubMed: 15671182]

25. Price LS, et al. Calcium signaling regulates translocation and activation of Rac. J. Biol. Chem. 2003; 278:39413–39421. [PubMed: 12888567]

26. Weiner OD, et al. A PtdInsP(3)- and Rho GTPase-mediated positive feedback loop regulates neutrophil polarity. Nat. Cell Biol. 2002; 4:509–513. [PubMed: 12080346]

27. van Haastert PJ, Keizer-Gunnink I, Kortholt A. Essential role of PI3-kinase and phospholipase A2 in Dictyostelium discoideum chemotaxis. J. Cell Biol. 2007; 177:809–816. [PubMed: 17535967]

28. Hawkins PT, et al. PDGF stimulates an increase in GTP-Rac via activation of phosphoinositide 3-kinase. Curr. Biol. 1995; 5:393–403. [PubMed: 7627555]

29. Claesson-Welsh L. Platelet-derived growth factor receptor signals. J. Biol. Chem. 1994; 269:32023–32026. [PubMed: 7798193]

30. Ware MF, Wells A, Lauffenburger DA. Epidermal growth factor alters fibroblast migration speed and directional persistence reciprocally and in a matrix-dependent manner. J. Cell Sci. 1998; 111(Pt 16):2423–2432. [PubMed: 9683636]
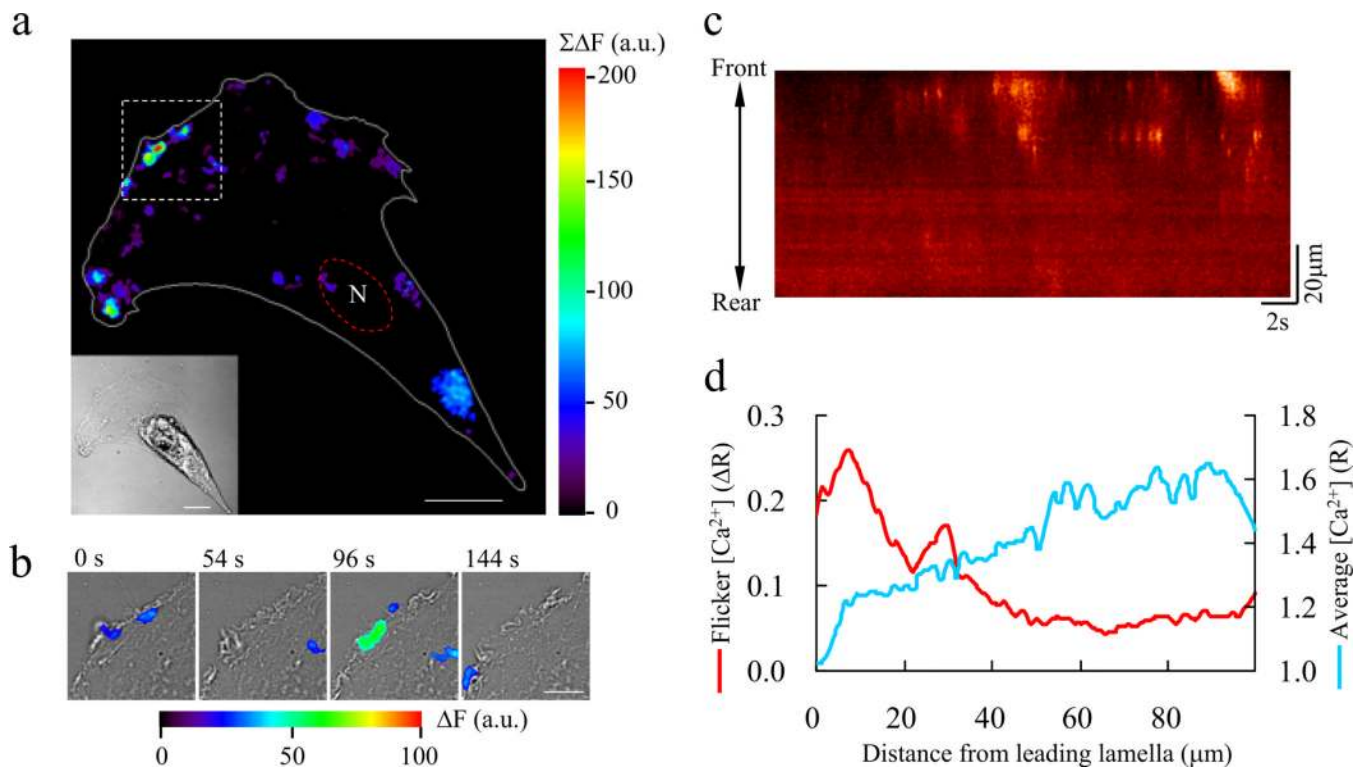
Figure 1. Calcium flickers in migrating fibroblasts
a. Calcium flickers. In a polarised WI-38 fibroblast (insert), local calcium increases ($\Sigma\Delta F$) were summed over 30 consecutive images acquired at 6 s intervals. "N" marks the nucleus. Scale bar: 15 μm. **b**. Calcium flickers (colour overlay) in motile lamellipodia (box in **a**). Scale bar: 5 μm. **c**. Polarisation of calcium flicker activity. The image consists of 10000 front-to-rear linescans, expressed as the ratio between fluo-4 and fura-red fluorescence (R). **d**. Opposing gradients of calcium flicker activity (ΔR) and global calcium (R, inclusive of flicker activity). Similar results were observed in eight cells.
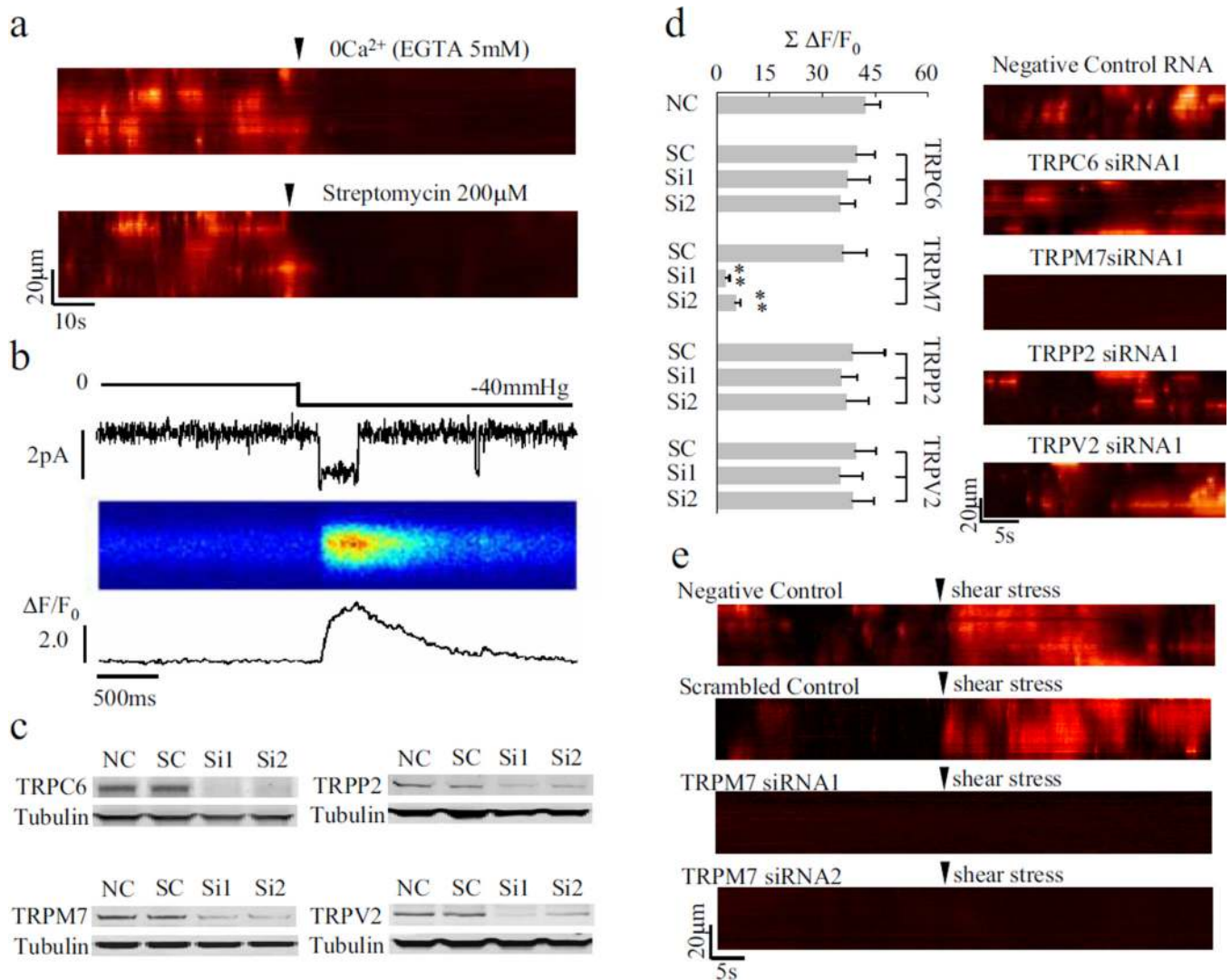
Figure 2. Triggering calcium flickers by TRPM7

a. Abolition of calcium flickers by streptomycin or removal of external calcium. **b**. Visualisation of calcium entry through single SACCs. From top to bottom: suction through the patch pipette, single-channel currents, and linescan image and line plot of local calcium transients. **c**. RNA interference knockdown of TRPC6, TRPM7, TRPV2 and TRPP2 assayed by Western blotting. NC, negative control RNA; SC: scrambled control RNA; Si1 and Si2, different siRNA sequences (see supplementary Table 2). **d**. Knockdown of TRPM7, but not TRPC6, TRPV2 or TRPP2, abolished calcium flickers. Data are expressed as mean±s.e.m.; n =12–21 cells in each group, **p < 0.01 *vs.* respective SC. **e**. TRPM7 knockdown prevented shear stress-induced calcium flickers.
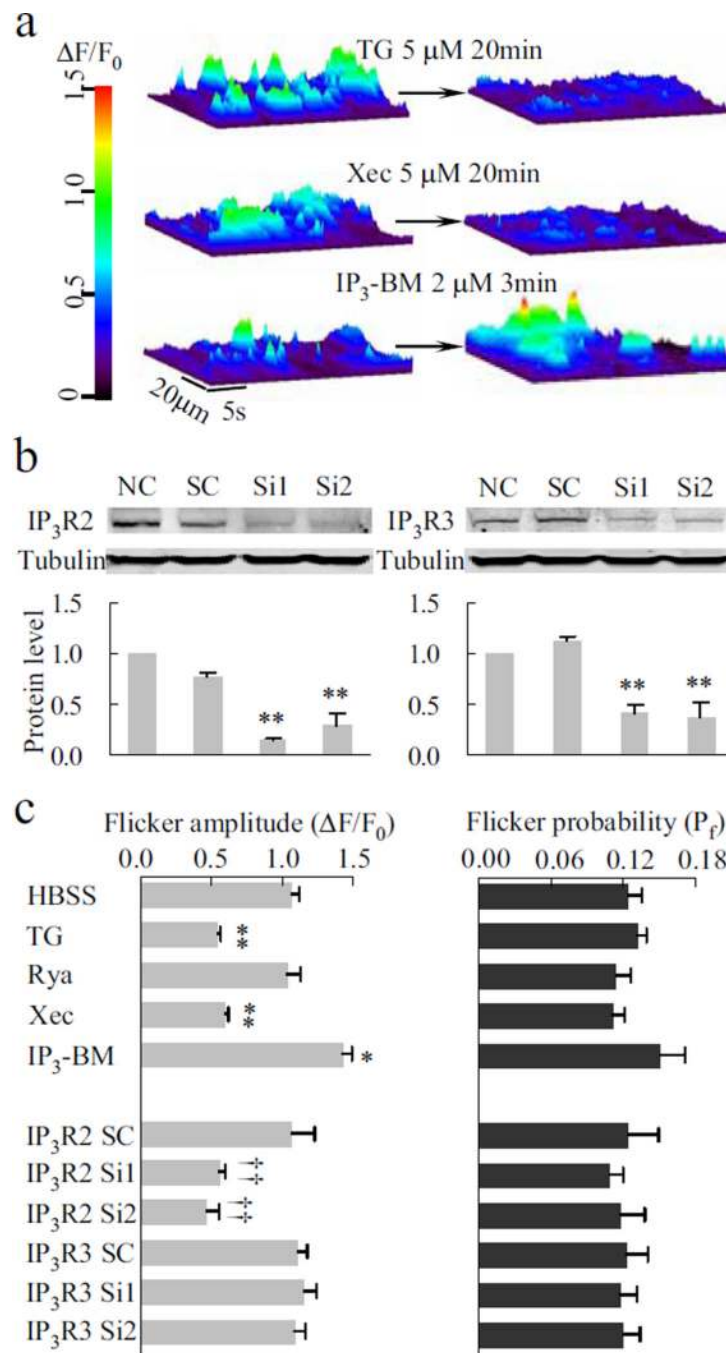
Figure 3. Amplifying TRMP7 calcium flickers by store calcium release through type 2 IP$_3$ receptors

a. Typical calcium flicker responses to thapsigargin (TG), xestospongin C (Xec) or IP$_3$-BM. Linescan data of $\Delta F/F_0$ are rendered as surface plots. **b**. Western blotting of IP$_3$Rs. See supplementary Table 2 for sequences of negative control (NC), respective scrambled control (SC), Si1 and Si2. Data are expressed as mean±s.e.m. (n=3–4). **p < 0.01 *vs.* respective SC. **c**. Flicker amplitude and probability under various experimental conditions. Pf: fractional time spent in calcium flickers; HBSS: Hepes-buffered saline solution; Rya: ryanodine (25μM, 15 min); n=10–29; *p < 0.05; **p < 0.01 *vs.* HBSS; ††p < 0.01 *vs.* respective SC.

Note that perturbing the ER calcium release mainly altered flicker amplitude without affecting flicker probability.
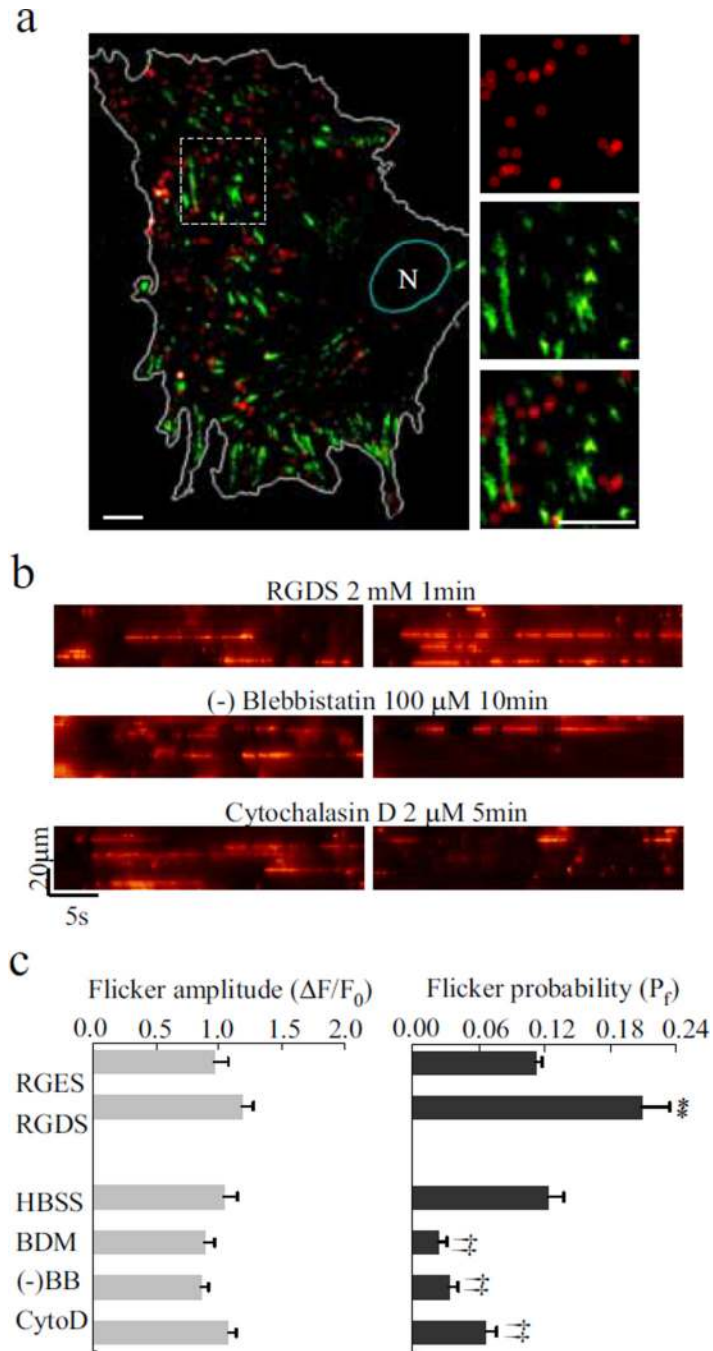
Figure 4. Traction force generation and calcium flicker activity
a. Maps for calcium flicker ignition sites (red dots) and FAs (green). FAs were visualized by immunostaining for integrin α5 after calcium flicker acquisition. Enlarged views of calcium flickers, FAs, and their overlay are shown to the right. "N" denotes the nucleus. Scale bar: 8 μm. **b**. Lamella flicker prior to (left) and after (right) application of compounds that affect traction force-generating elements. **c**. Statistics of calcium flicker amplitude and probability (Pf). HBSS, Hepes-buffered saline solution; BDM, 2,3-butanedione monoxime (10 mM); (−)BB, (−)blebbistatin (100 μm); cytoD, cytochalasin D. Error bars represent s.e.m.; n = 10–19 in each group. **p < 0.01 *vs.* RGES; ††p < 0.01 *vs.* HBSS. Note that flicker probability

rather than amplitude was preferentially altered by varying the traction force, in contrast to the situation shown in Fig. 3.
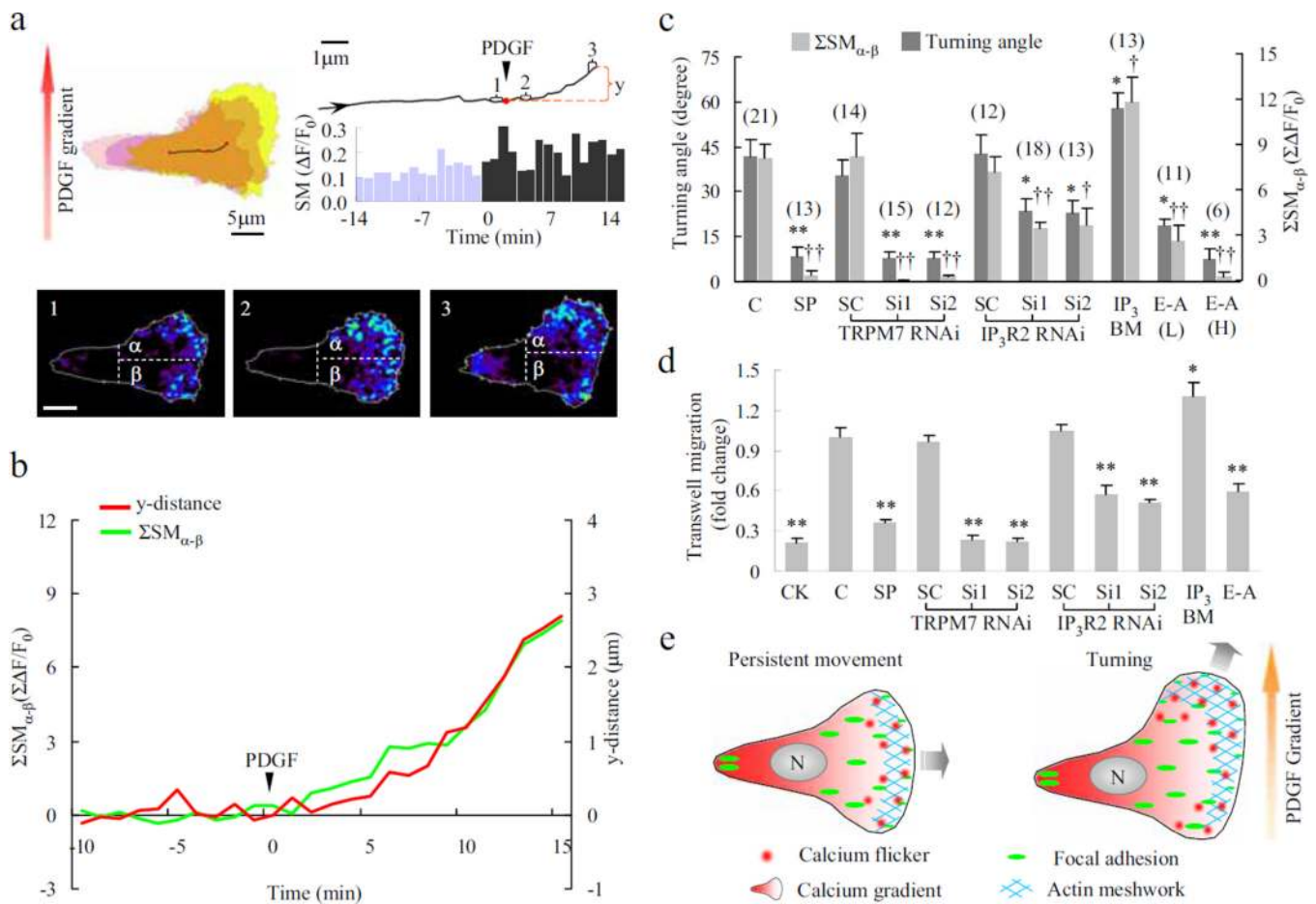
Figure 5. Calcium flickers steer fibroblast turning

a. Asymmetrical lamella flicker activity induced by a PDGF gradient. Upper left, contours of the cell border at -14 (pink), 0 (purple) and 15 min (yellow). Upper right, trajectory of the centre of the cell and time course of calcium flicker production (bar graph). "SM": signal mass of calcium flickers within the lamella. Lower panels: overlays of calcium flickers in 1-min windows (labelled 1–3 in the trajectory above). Dashed lines bisect the leading lamella into upper (α, facing the PDGF source) and lower portions (β) **b**. Correlation between cumulative asymmetric flicker activity ($\Sigma SM_{\alpha-\beta}$) and displacement along the PDGF gradient (y-distance). **c**. Relationship between turning angle and $\Sigma SM_{\alpha-\beta}$ (at 15 min). C, control with no treatment; SP, streptomycin 200 μM; Si1, Si2 and SC: two siRNA constructs and a scrambled control; IP_3-BM 2 μM; E-A, EGTA-AM, L, 2 μM, H, 20 μM. Data are expressed as mean±s.e.m.; "n" values are shown in parentheses. *$p < 0.05$; **$p < 0.01$ vs. turning angle of control or respective SC; †$p < 0.05$; ††$p < 0.01$ vs. $\Sigma SM_{\alpha-\beta}$ of control or respective SC. **d**. Chemotaxis of WI-38 fibroblasts. CK, chemokinesis assay with the same concentration of PDGF-BB on both sides of the well; E-A, EGTA-AM (2 μM). n=4–10, *$p < 0.05$; **$p < 0.01$ vs. control or respective SC. **e**. Cartoons of patterned calcium flicker activation in persistently moving (left) and turning fibroblasts (right). Calcium flicker activity during persistent movement displays a front-to-rear polarisation, opposing a rear-to-front global calcium gradient. During turning, calcium flicker activity becomes asymmetric across the leading lamella, in addition to enhanced flicker frequency and accentuated front-to-rear polarisation.